

Power scaling of a side-pumped Nd:YLF laser based on DBMC technology

Niklaus U. Wetter · Alessandro M. Deana

Received: 4 April 2014 / Accepted: 9 July 2014 / Published online: 22 July 2014
© Springer-Verlag Berlin Heidelberg 2014

Abstract This work demonstrates the power scalability of double-beam-mode controlling, a technique that has generated the highest optical efficiency reported so far for Nd:YLF lasers. We analyze two types of power scaling possibilities by numerical simulations: multiplication of intracavity pump modules and MOPA configuration. About 44 W of TEM₀₀ output power at 1053 nm was experimentally demonstrated with a beam-parameter product of 1.07×1.15 . The results show great ease of power scaling without sacrificing beam quality.

1 Introduction

Efficient and power-scalable diode-pumped solid-state laser designs (DPSSL) that operate in the fundamental transversal mode are fast becoming one of the main players in solid-state laser sales that, for industrial applications alone, already represent a US\$ 1.7 billion market [1]. Several different solid-state laser host materials [2–5] are capable of delivering efficient laser action of which YLiF₄ (YLF) has some unsurpassed characteristics that are vital to many applications. In particular, the weak thermal lensing, natural birefringence, and long upper-laser-level lifetime are important for good beam quality and many applications

such as Q-switching [6–9]. Moreover, the emission line at 1053 nm is of great interest for master oscillators of Nd:glass amplifiers [10].

When analyzing current cavity designs from the stand point of efficiency and beam quality, end-pumped geometries are indicated because with this design, the directional emission of the pump diodes allows for a good overlap between the laser's fundamental mode of oscillation and the pump beam. As a result, very high efficiencies with diffraction-limited beam quality can be achieved. The highest optical-to-optical efficiency of 50 %, reported for an end-pumped Nd:YLF, was achieved for the 1,047 nm emission line (which has a higher emission cross section than the 1,053 nm transition) by end-pumping the crystal with 2 W from a Ti:sapphire laser [11]. However, the requirement of power scalability cannot be fulfilled easily with end-pumped lasers, and expensive and cumbersome measures need to be used in order to increase their output power [12].

Side-pumped designs spread the pump power over a wider active area decreasing pump intensity and allowing for more pump power to be delivered into the active medium. The main drawback of this architecture is its non-collinearity between pump and emission, which usually results in incomplete pump overlap and multimode operation [13]. One exception to the usually low efficiency in side-pumped lasers is an architecture based on gain media with high absorption cross section, such as Nd:YVO₄ and Nd:GdVO₄, where the shallow region of pump-induced inversion gets efficiently screened by a single-grazing incidence beam that undergoes total internal reflection (TIR) at the pump surface [14].

For Nd:YLF, a single bounce at the pump facet of this active medium does result in inefficient or multimode operation due to the lower absorption coefficient of the

N. U. Wetter (✉)
Center for Lasers and Applications, Instituto de Pesquisas
Energéticas e Nucleares - IPEN, 2242 Av. Prof. Lineu Prestes,
São Paulo, Brazil
e-mail: nuwetter@ipen.br

A. M. Deana
Department of Biophotonics Applied to Health Sciences,
Universidade Nove de Julho - UNINOVE, 235 Vergueiro St,
São Paulo, Brazil

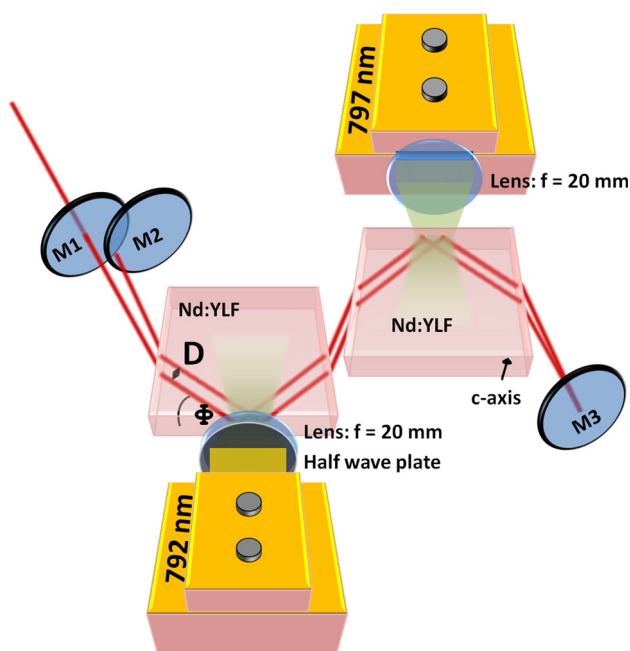


Fig. 1 Schematic diagram of the DBMC-amplified laser design

crystal [13]. Therefore, in order to solve the limitations of current technologies, a double-beam method with two TIR was developed, dubbed double-beam-mode controlling (DBMC), to achieve better overlap. This technique introduces a third mirror into the cavity that displaces the position of the second laser beam with respect to the first beam, making an offset second pass through the active medium (Fig. 1). The controlled gain competition between the two near-parallel beams inside the slab guarantees stable TEM₀₀ mode operation at high pump powers, without inserting additional losses [15, 16]. No cylindrical intracavity optics is needed to create the highly elliptical beams necessary with other techniques [14].

DBMC has proven to be capable of delivering a diffraction-limited laser beam with up to 53.6 % of optical-to-optical efficiency (63.5 % slope efficiency) which is the highest optical efficiency ever reported for a Nd:YLF laser pumped around 800 nm, including multimode operation, operation at the higher gain line (1047 nm), and end-pumped schemes [15]. In this work, we demonstrate, for the first time, the power scalability of this technique by introducing the two different gain crystals side by side into the cavity.

2 Experimental setup

Figure 1 shows a schematic diagram of the laser setup.

Both a-cut crystals had 1 mol % of neodymium doping level. Their dimensions were $13 \times 13 \times 3 \text{ mm}^3$, and their

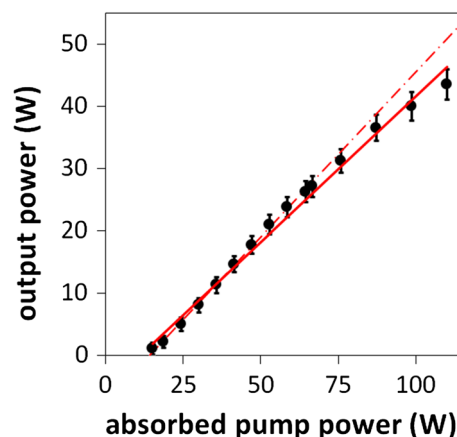


Fig. 2 Output power as a function of pump power for an output coupler with 20 % transmission. The solid line represents a linear regression considering all experimental data, and the dashed line of 53 % slope represents a linear regression considering only pump powers up to 64 W

c-axis was oriented perpendicular to the large cooling facets. The crystals were placed on a copper plate without any further cooling system. Pulse duration was kept at 1 ms, and the duty cycle was below 5 % to avoid thermal fracture. Two qcw diode bars were used as pump sources. One had its peak emission at 792 nm when operated at 27° C and required an additional half wave plate after the fast-axis collimating lens to rotate the polarization of the output beam by 90° in order to access the crystal's highly absorbing π -polarization. The other diode had a peak emission at 797 nm when operated at 19° C. Both diode beams were focused into the two crystals by a $f = 20 \text{ mm}$ spherical lenses, resulting in spot sizes of approximately 4 mm width and 0.1 mm height. At 40 A of drive current, the diodes showed a spectral emission width of 2 nm FWHM, which increased at higher currents by 26 % [17]. After the focusing optics and Fresnel reflections at the uncoated pump facets, about 88.5 % of the pump power was effectively absorbed by the slabs. The cavity was further composed by two highly reflecting mirrors, one flat (M2) and one curved mirror (M3) with 10 m radius of curvature (ROC). Even though the laser was very compact, the long ROC of the curved mirror does allow to increase the optical length of the laser up to a few meters without instability, as required for example for mode-locking operation. The transmission of the flat output coupling mirror (M1) was varied from 5 to 25 %.

3 Results

The laser threshold was 12.9 W of pump power and the maximum power fluctuation, after a few minutes of warm-

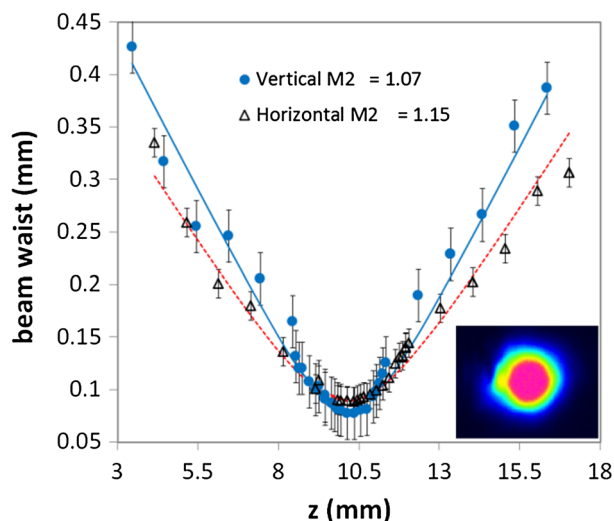


Fig. 3 Beam profile and M^2 measurements of the DBMC laser. The inset shows the laser beam after the output coupler as measured with a CCD

up time, was less than 2 % over a test period of 4 h. Optimum results were obtained by using a 20 % transmission output coupler at 1053 nm. At the maximum available absorbed pump power of 110 W, the output power was 44 W with diffraction-limited beam quality and slightly decreased optical-to-optical efficiency of 42 %. The slope efficiency of the laser was 46 % (solid line fit of Fig. 2). Even in the absence of significant heat load, a weak rollover of the output power was observed in Fig. 2. This occurs because beyond 80 W of pump power (40 A of diode current) the diodes suffer a spectral broadening as pointed out above and in Ref. [17].

The DBMC architecture requires a well-matched effective absorption coefficient and laser beam size inside the crystal in order to efficiently screen the population inversion. The spectral broadening of the diodes increases the penetration depth, resulting in a poorer overlap between the fundamental mode of the laser oscillation and the pump beam. Therefore, the laser output power and, consequently, its efficiency are decreased [17]. This effect is especially detrimental to the 797 nm emitting diode, because the Nd:YLF absorption peak at this wavelength is 21 % narrower than the 792 nm absorption peak. Extrapolation of the experimental data at lower pump powers (Fig. 2, dashed line) demonstrates that, without the spectral broadening, a slope efficiency of 53 % is possible.

Caird's analysis was carried out and resulted in resonator losses of 7.5 ± 2 %. The high losses are attributed to sixteen air/crystal interfaces and eight total internal reflections at the pump facets that the beam undergoes during each round-trip. The average loss per interface is

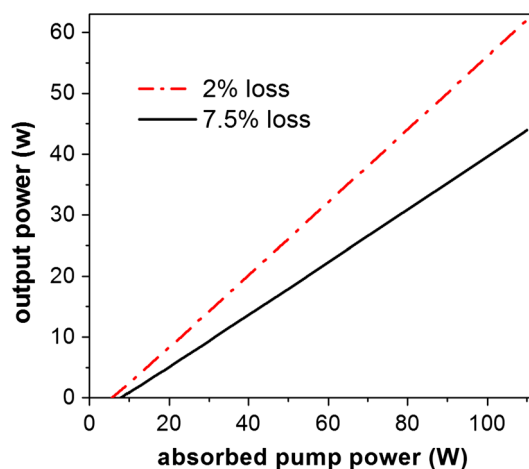


Fig. 4 Simulated output power as a function of pump power for 2 % of losses (dotted line) and 7.5 % of losses

only 0.3 %. Therefore, better results can be expected if the two crystals are substituted by one single, twice as large crystal.

Figure 3 shows the measurements of the beam profile along with the M^2 fit of the laser beam. M^2 values of 1.15 and 1.07 were obtained in the horizontal and vertical directions, respectively. The excellent beam quality demonstrates that even at very high intracavity powers, multi-mode oscillation is avoided by the DBMC technique, which is equivalent to a soft aperture for higher modes [17].

4 Simulations

We extensively simulated the transition from one pump module to two pump modules in order to find out which configuration would give the best results for power scaling. In the first part of this section, we demonstrate the results for two modules inside the same cavity, a design that clearly fares better than the MOPA design simulated in the second part.

By inserting another crystal inside the cavity, pumped by a second identical diode, one effectively doubles the overlap volume between pump-generated inversion and laser beam without increasing the inversion density. As a consequence, if the geometrical pump and laser beam parameters can be maintained and if the losses remain the same, no change in slope efficiency is expected and twice as much output power should be obtained for two pump modules when compared to a single pump module (a low threshold is assumed). This agrees well with the results obtained in this research that is double the output power of previous publications using single pump modules [15].

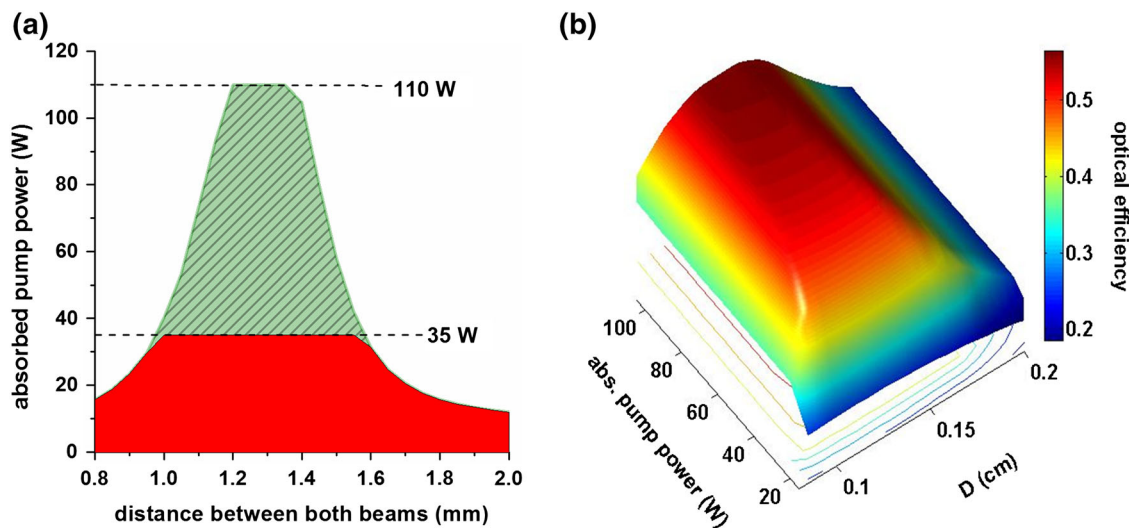


Fig. 5 **a** Pump power and beam separations D for one pump module (solid fill area only) and two pump modules (solid and patterned area) at which fundamental mode output is achieved. **b** Efficiency as a function of beam separation and pump power

The laser was simulated in detail and optimized in terms of resonator geometry, diode characteristics, crystal shape, and doping level, using a space-dependent MATLAB code, which was developed using a theoretical model based on [18]. This code calculates the output power and the threshold of higher-order transversal modes, as a function of overlap between spatial population inversions and laser mode distributions. The output power as a function of absorbed pump power for different resonator losses is shown in Fig. 4.

The simulation of the output power as a function of absorbed pump power demonstrates clearly the importance of reducing the losses: With 7.5 % of losses, the simulated output power, slope efficiency, and optical-to-optical efficiency at 110 W of absorbed pump power are 43.9 W, 43, and 39.9 %, respectively. This is in good agreement with the measured values (44 W and 42 % optical efficiency). For 2 % of losses, the same parameters read 62.1 W, 60 and 56.5 %, respectively.

As pointed out above, the slope efficiency should remain the same for one or two modules. The calculated 60 % slope efficiency is smaller than for one single module as reported earlier (63 %, Ref. [15]). This lower slope efficiency is because one of the two diodes, in the otherwise identical double pump setup, emits at 797 nm and therefore has lower absorption efficiency as already discussed above.

As stated in the introductory part and explained in detail in References [5, 9, 15], the gain competition between the two near-parallel beams inside the slab, necessary for TEM_{00} mode operation, is controlled primarily by the adjustment of the distance D between both beams (see Fig. 1). As the pump power increases, the population inversion becomes stronger in regions that are not screened

by the fundamental transverse mode and the laser may start to oscillate in the next higher-order mode. The range of separations D between both beams, for which operation in fundamental transverse mode is maintained, is therefore expected to decrease as a function of pump power (see Fig. 5a).

Figure 5a shows combinations of pump powers and beam separations at which fundamental mode is achieved for one pump module and two pump modules. In both cases, all other parameters of the cavity are exactly the same and as in Ref [15]. Maximum assumed pump power is 35 W [15] for one module and 110 W for two modules (this work). As can be seen in Fig. 5a), at 35 W of pump power, the cavity remains stable for beam separations D ranging from 1 to 1.6 mm. However, at 110 W of absorbed pump power, the same interval decreased by 2/3: TEM_{00} is only possible from 1.2 to 1.4 mm. The simulations show that a limit is reached for 140 W of pump power when the cavity becomes multimode. In order to overcome this pump power limit, the cavity parameters need to be changed, for example, by increasing the TEM_{00} mode size. Figure 5b shows the optical efficiency as a function of pump power. Again, clearly demonstrated is the fact that for higher pump powers, the range of separations D at which TEM_{00} operation works is smaller. As expected, a slight increase in optical efficiency is achieved at higher pump powers.

4.1 Comparison with MOPA design

Power scalability of DPSSL is often obtained by applying a technique known as master oscillator power amplifier (MOPA). In this configuration, a master laser's (or seed

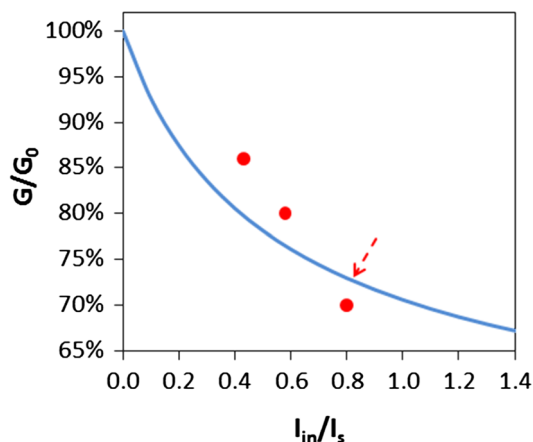


Fig. 6 Net normalized amplifier gain. The *solid curve* uses always the same unsaturated gain G_0 measured in Ref [15]. *Dots* are generated using the simulation software which calculates saturated (G) and unsaturated gain (G_0) for each value of I_{in}/I_s . The *arrow* corresponds to a beam radius at the amplifier of 0.55 mm as used in our experiment

laser’s) signal is boosted by an external optical amplifier [19]. MOPAs are especially suited for the amplification of high-energy short pulses that cannot be resonated inside an oscillator because the high intracavity intensity would destroy the coatings or for the case of amplification of single-frequency lasers that operate only in single mode if they operate very little above threshold.

In a first simulation, a single-pass MOPA is calculated in order to see whether this simple configuration could generate better results than our cavity of Fig. 1 [20]. In a single-pass MOPA configuration, the high intracavity losses experienced in our setup with two separate crystals (results, Sect. 3) can be in part avoided, which should lead to a better overall performance. A simple model for the relation between the small-signal gain and saturated gain for steady-state amplification is derived in Ref. [19] and is shown in Eq. (1)

$$\frac{I_{in}}{I_s} = \frac{\ln(G_0/G)}{G - 1} \tag{1}$$

where $G_0 = \exp(g_0l)$ is the small-signal, single-pass gain for an amplifier of length l . I_{in} is the intensity at the entrance facet of the amplifier module. I_s is the saturation intensity of 2473 W/cm² (sigma emission at 1053 nm). $G = I_{out}/I_{in}$ is the saturated gain. It is assumed for the following calculation that the crystal in the master oscillator is pumped by half the total absorbed pump power (55 W) used in our experiment and that the second crystal in the amplifier is pumped by the other half, in an otherwise identical setup, keeping therefore the total pump power

equal in both experiments. The output power from the master oscillator is 28 W at 55 W of pump power, as retrieved from Fig. 4 (dotted curve). Further, we assume that the losses in the amplifier are 2 %, and all parameters of the master oscillator are as in Ref. [15] (except pump power). These small losses in the amplifier, as opposed to the 7.5 % losses measured in our experiment, should, in principle, give an advantage to the MOPA configuration.

For the theoretical curve of equation (1) in Fig. 6, we used the small-signal gain measured in Ref. [15], $G_0 = 1.9$, which uses a beam radius of 0.55 mm at the crystal location ($I_{in}/I_s = 0.8$). This measured value of G_0 agrees very well with the result from the simulation, $G_0 = 1.96$, using the space-dependent MATLAB code. For other values of the beam radius at the amplifier, which affects I_{in} , we used the values of G and G_0 calculated by the program (dots in Fig. 6).

As seen in Fig. 6, a higher net normalized amplifier gain is achieved for larger beam radii. The size of the beam at the entrance of the amplifier is limited by the physical size of the Nd:YLF slab which is 3 mm in height. Therefore, assuming that the onset of diffraction losses at the border of the crystal occurs for a beam mode size half as big as the dimension of the crystal [19], the maximum beam radius is 0.75 mm which translates into a ratio of $I_{in}/I_s = 0.43$. For this value, a ratio of $G/G_0 = 0.86$ is obtained (leftmost dot in Fig. 6), which, together with the value of the corresponding calculated small-signal single-pass gain of $G_0 = 1.57$, results in an amplification of 36 %. The final output power of the simulated single-pass MOPA configuration is therefore 38 W, which is less than the 44 W of output power simulated (Fig. 4) and measured (Fig. 2) with the cavity of Fig. 1 in agreement with the previous experiments [20].

Multi-pass amplification was also simulated. From a practical point of view, one should refrain from using very large beams such as the 0.75 mm beam simulated before, because the slightest misalignment will cause large diffraction losses. A 0.55-mm beam radius will suffer amplification of 45, 49, and 50 % for two, three, and four passes, respectively, through the amplifier. Although this setup would be fairly easy to implement, because the output beam from the master oscillator of our setup has approximately the same radius, the final output power of 42 W is still less than in our cavity (Fig. 1). A good compromise for the MOPA is achieved using a beam radius of 0.65 mm: With three passes through the amplifier, more than 45 W of output power should be achieved. However, the complexity of the three-pass MOPA is rather high when compared to the present, simple cavity design because additional mirrors and beam-conforming optics are required.

5 Conclusions

About 44 W of laser output power at 1053 nm was obtained at a slope efficiency of 46 %. The simulation demonstrates that 60 % slope efficiency is possible with fewer losses, as expected by substituting the two crystals by one single, twice as large crystal. Simulation showed that placing the second laser crystal inside the resonator results in 57 % amplification of the laser power, which was confirmed by the experiment, whereas an optimized single-pass MOPA amplifier would result in only 36 % of amplification. This demonstrates clearly the usefulness of power scaling DBMC lasers. Additionally, the traditionally excellent beam quality of Nd:YLF lasers can be maintained during power scaling as shown by the M^2 measurement of 1.1 average, obtained in this work.

Acknowledgments The authors gratefully acknowledge FAPESP and CNPq for the financial support for this work.

References

1. D.A. Belfort, Status-quo for 2013. *Ind. Laser Sol.* **28**, 1 (2013)
2. E.J. Hao, T. Li, Z.D. Wang, Y. Zhang, Nd:GdVO₄ ring laser pumped by laser diodes. *Laser Phys. Lett.* **10**, 025803 (2013)
3. L.B. Su, Q.G. Wang, H.J. Li, G. Brasse, P. Camy, J.L. Doualan, A. Braud, R. Moncorgé, Y.Y. Zhan, L.H. Zheng, Spectroscopic properties and CW laser operation of Nd, Y-codoped CaF₂ single crystals. *Laser Phys. Lett.* **10**, 035804 (2013)
4. F. Li, J. Wang, H. Zang, M. Huang, W. Chen, Single-frequency Q-switched double-pulse Nd:YAG laser. *Laser Phys. Lett.* **10**, 035001 (2013)
5. N.U. Wetter, F.A. Camargo, E.C. Sousa, Mode-controlling in a 7.5 cm long, transversally pumped, high power Nd:YVO₄ laser. *J. Opt. A Pure Appl. Opt.* **10**(10), 104012 (2008)
6. A.M. Deana, N.U. Wetter, High-efficiency, Q-switched and diffraction-limited Nd:YLF side-pumped laser. *Proc. SPIE* **8433**, 84330B (2012)
7. Y. Sun, H. Zhang, Q. Liu, L. Huang, Y. Wang, M. Gong, Efficient and compact diode-end-pumped conductively cooled Q-switched Nd:YLF laser operating at 527 nm. *Laser Phys. Lett.* **7**, 722–725 (2010)
8. A.M. Deana, E.C. Sousa, I.M. Ranieri, S.L. Baldochi, N.U. Wetter, 1 kHz repetition rate, mode-controlled, passively Q-switched Nd:YLF laser operating at 1,053 nm. *Proc. SPIE* **8235**, 82350G (2012)
9. A.M. Deana, I.M. Ranieri, S.L. Baldochi, N.U. Wetter, Compact, diode-side-pumped and Q-switched Nd:YLiF₄ laser cavity operating at 1053 nm with diffraction limited beam quality. *Appl. Phys. B. Laser Opt.* **106**, 877–880 (2012)
10. A.V. Okishev, W. Seka, Diode-pumped Nd:YLF master oscillator for the 30-kJ (UV), 60-beam OMEGA laser facility. *IEEE J. Sel. Top. Quantum Electron.* **3**(1), 59–63 (1997)
11. Y.F. Lue, X.H. Zhang, A.F. Zhang, X.D. Yin, J. Xia, Efficient 1,047 nm CW laser emission of Nd:YLF under direct pumping into the emitting level. *Opt. Commun.* **283**, 1877–1879 (2010)
12. E.H. Bernhardt, A. Forbes, C. Bollig, M.J.D. Esser, Estimation of thermal fracture limits in quasi-continuous-wave end-pumped lasers through a time-dependent analytical model. *Opt. Express* **16**, 11115–11123 (2008)
13. N.U. Wetter, E.C. Sousa, F.A. Camargo, I.M. Ranieri, S.L. Baldochi, Efficient and compact diode-side-pumped Nd:YLF laser operating at 1,053 nm with high beam quality. *J. Opt. A: Pure Appl. Opt.* **10**, 104013 (2008)
14. A. Minassian, B. Thompson, M.J. Damzen, Ultrahigh-efficiency TEM₀₀ diode-side-pumped Nd:YVO₄ laser. *Appl. Phys. B* **76**, 341–343 (2003)
15. N.U. Wetter, A.M. Deana, Diode-side-pumped Nd:YLiF laser emitting at 1,053 nm with 53.6% optical efficiency and diffraction-limited beam quality. *Laser Phys. Lett.* **10**, 035807 (2013)
16. N.U. Wetter, E.C. Sousa, I.M. Ranieri, S.L. Baldochi, Compact, diode-side-pumped Nd³⁺:YLiF₄ laser at 1,053 nm with 45% efficiency and diffraction-limited quality by mode controlling. *Opt. Lett.* **34**, 292–294 (2009)
17. A.M. Deana, M.A.P.A. Lopez, N.U. Wetter, Diode-side-pumped Nd:YLF laser emitting at 1,313 nm based on DBMC technology. *Opt. Lett.* **38**, 4088–4091 (2013)
18. K. Kubodera, K.J. Otsuka, Single-transverse-mode LiNdP₄O₁₂ slab waveguide laser. *Appl. Phys.* **50**, 653–659 (1979)
19. W. Koechner, *Solid-state laser engineering* (Springer, Berlin, 2006)
20. F. Peter, *Moulton* (Diode Laser Technology Review, Boston, 1998)